HiSST: International Conference on
High-Speed Vehicle Science Technology
26–29 November 2018, Moscow, Russia

Assessment of VTVL and VTHL Reusable First Stages

L. Bussler[1], J. Wilken, S. Stappert, M. Sippel, I. Dietlein, E. Dumont

Abstract

Two-stage vertical take-off vertical landing (VTVL) and vertical take-off horizontal landing (VTHL) partially reusable launcher configurations are systematically analyzed. The investigated configurations consider a reusable first stage that either performs a landing at the launch site (return to launch site RTLS) or a landing downrange of the launch site (downrange landing DRL). The considered propellant combinations include LOX/LH2, LOX/LCH4 and LOX/RP-1. Configurations based on staged combustion and gas generator cycle engines are analyzed. The same engines however with different expansion ratios are used on the reusable first stages and the expendable upper stages. Special emphasis is put on analyzing the different configurations under similar design assumptions that allow a comparison of gross lift-off masses, stage lift-off masses, stage structural indices as well as loads encountered by the reusable stages during atmospheric reentry. Based on this comparison benefits and drawbacks of the investigated RLV configurations are discussed.

Keywords: *VTVL, VTHL, RLV*

Acronyms

AoA	Angle of Attack
DRL	Down Range Landing
FB	Fly-Back
GG	Gas Generator
GLOM	Gross Lift-Off Mass
IAC	In-Air-Capturing
LCH4	Liquid Methane
LH2	Liquid Hydrogen
LOX	Liquid Oxygen
RCS	Reaction Control System
RLV	Reusable Launch Vehicle
RP-1	Rocket Propellant 1 (Kerosene)
RTLS	Return To Launch Site
SC	Staged Combustion
TPS	Thermal Protection System
VTHL	Vertical Take-Off Horizontal Landing
VTVL	Vertical Take-Off Vertical Landing

Nomenclature

Isp	-	Specific impulse	[s]
L/D	-	Lift-to-drag ratio	[-]
T/W	-	Thrust-to-weight ratio	[-]
ΔV	-	Delta velocity	[m/s] or [km/s]
γ	-	Flight path angle	[°]
ε	-	Expansion ratio	[-]

[1] *DLR Institute of Space Systems, Robert-Hooke-Straße 7 28359 Bremen Germany, Leonid.Bussler@dlr.de*

1. Introduction

The goal of the performed analysis is to assess different partially reusable space transportation systems ensuring maximum comparability of the configurations while maintaining similar requirements w.r.t. launch site, target orbit and payload mass. This should allow making a contribution to the ongoing discussion about RLV in the space transportation community in general and to the definition of potential configurations for a possible future European launch vehicle in particular. The presented work is part of the ENTRAIN (European Next Reusable Ariane) system study, [1], [2] and [3]. While the consideration of RLV in Europe in the area of VTVL is driven by recent achievements of Space X and Blue Origin in the United States, one of the most detailed investigations in the area of VTHL performed in the past in DLR in cooperation with German industry has been the ASTRA Liquid Fly-Back Booster (LFBB), [4], Fig 1.

Fig 1. ASTRA LFBB artists' impression, [4]

The systematic study performed within DLR and presented in this paper considers different types of recovery methods. The winged fly-back (FB) boosters perform an unpowered atmospheric reentry after separating from the upper stage and return to launch site performing a subsonic cruise flight with on-board air-breathing engines. Amongst others reusable first stage separation velocity, stage mass and the distance to launch site determine the necessary thrust of air-breathing engines and fly back fuel mass. Accounting for the drawback of the fly back booster concept to carry its fly-back fuel mass during the ascent as well as the descent part of the trajectory the so called In-Air-Capturing (IAC) method attempts to achieve smaller, lighter reusable stages by towing the winged vehicles back to launch site by means of an aircraft, see [5] and [6]. The general approach is illustrated in Fig 2.

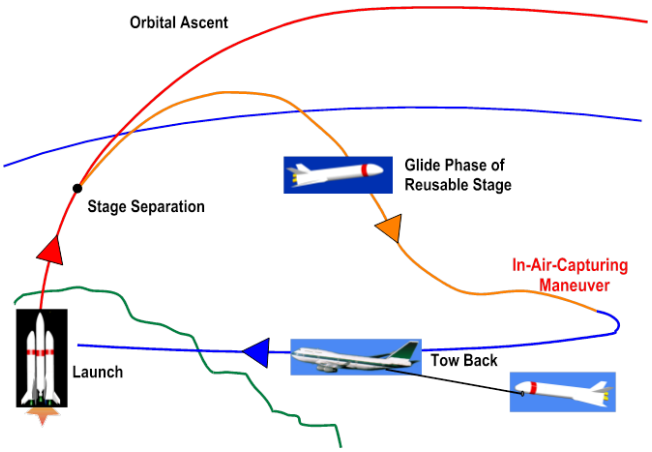

Fig 2. In-Air-Capturing method for winged boosters, [5]

The reusable unpowered stage is approaching the airliner from above actively controlled by aerodynamic braking. After successful connection of both vehicles, the winged reusable stage is towed back to the launch site. Close to the airfield, the stage is released and autonomously glides like a sailplane to earth.

In contrast to winged stages VTVL concepts rely on rocket engines for decelerating and landing the reusable first stage. Both down range landing as well as a return to launch site are possible. In case of RTLS the first stage performs a so called toss-back maneuver in order to modify its velocity vector

and redirect the trajectory towards the launch site. The toss-back maneuver is followed by a number of propulsive and non-propulsive phases. Non-propulsive phases within the atmosphere are controlled aerodynamically. A final landing burn is performed during the vertical landing close to the launch site. In case of DRL the engine is used only in order to decrease the velocity and related mechanical and thermal loads on the vehicle during the descent (reentry burn) and perform the vertical landing. No propellant is consumed for the return to the launch site. Example trajectories of VTVL configurations are shown in Fig 3.

Fig 3. VTVL RTLS and DRL trajectories. First stage ascent = dark green, upper stage ascent = yellow, RTLS toss-back = red, non-propulsive phase prior to reentry burn = blue, reentry burn = magenta, non-propulsive phase prior to landing burn = light green, [1]

While one objective of this paper is a synthesis and comparison of the different available return options for reusable first stages increased attention is drawn towards winged reusable first stages including such aspects as reusable first stage ascent and descent trajectory, aerodynamics and thermal protection system mass estimation. Investigations of VTVL and VTHL configurations in DLR are summarized in [1], [3], [6] - [9]. Recent investigations concerning IAC can be found in [6].

2. General Study Assumptions

The following parameters are considered important to obtain comparable reusable first stages: thrust-to-weight ratio (T/W) at launch and upper stage delta velocity (ΔV). A T/W of 1.4 is fixed for all configurations. Upper stage ΔVs of 6.6, 7.0 and 7.6 km/s are considered for hydrogen staged combustion VTHL configurations. The upper stage ΔV range of interest for VTVL stages has been narrowed down in [1] and [3]. For the presented work upper stage delta velocities of 7.0 km/s are considered for VTVL hydrogen staged combustion and gas generator as well as methane and kerosene gas generator configurations. VTHL configurations for the aforementioned propellant and engine cycle combinations are also designed for an upper stage ΔV of 7.0 km/s. The necessary upper stage ΔV is considered to be a more precise way to compare different configurations than e.g. reusable first stage separation Mach number (which would be influenced by the specific ascent trajectory and separation altitude), [1]. The above ΔV values refer to actual changes in velocity during powered flight. Another important aspect is the assumption of the same fuel/oxidizer combination for the reusable first stages and the expendable upper stages. Also the same type of engine with different expansion ratios ε is used for the lower and upper stage. The number of stages is set to two for all analyzed configurations regardless of the propellant combination. Tandem staging is used for all configurations. The propellant tanks of the reusable first stage as well as the expendable upper stage are common bulkhead tanks.

The principal study assumptions are summarized below:

- Reference mission: delivery of 7000 kg + 500 kg project margin to GTO
- Two stage, tandem staging configurations
- Geostationary Transfer Orbit (GTO) parameters: 250 km × 35786 km, 6° inclination
- Launch site: Kourou, French Guyana, 52.77° W / 5.24° N

For RLV stages a system mass margin of 14% is applied to all components except the propulsion subsystem. For expendable upper stages a margin of 10% is applied to all components except the propulsion subsystem. For components of the propulsion subsystem a margin of 12% is applied for both RLV and expendable stages. Propellant reserves of 0.9% relative to the ascent – in case of VTVL also descent – propellant mass are foreseen for all fuel/oxidizer combinations. In addition a propellant reserve of 20% is foreseen for the cruise flight towards the launch site for winged fly-back boosters.

The following return options are considered:

- Winged fly-back booster – VTHL/RTLS
- Winged booster, In-Air-Capturing – VTHL/DRL
- Non-winged stage performing a down range landing – VTVL/DRL

It should be noted that in-Air-Capturing is categorized here as DRL since – from an RLV stage performance point of view – this return method is equivalent to a landing down range of the launch site without return flight.

3. Preliminary Design of VTVL and VTHL Configurations

Below the preliminary design of the VTVL and VTHL configurations as well as the applied methods are described. Specific aspects of VTVL and VTHL preliminary design are discussed.

3.1. General Architecture

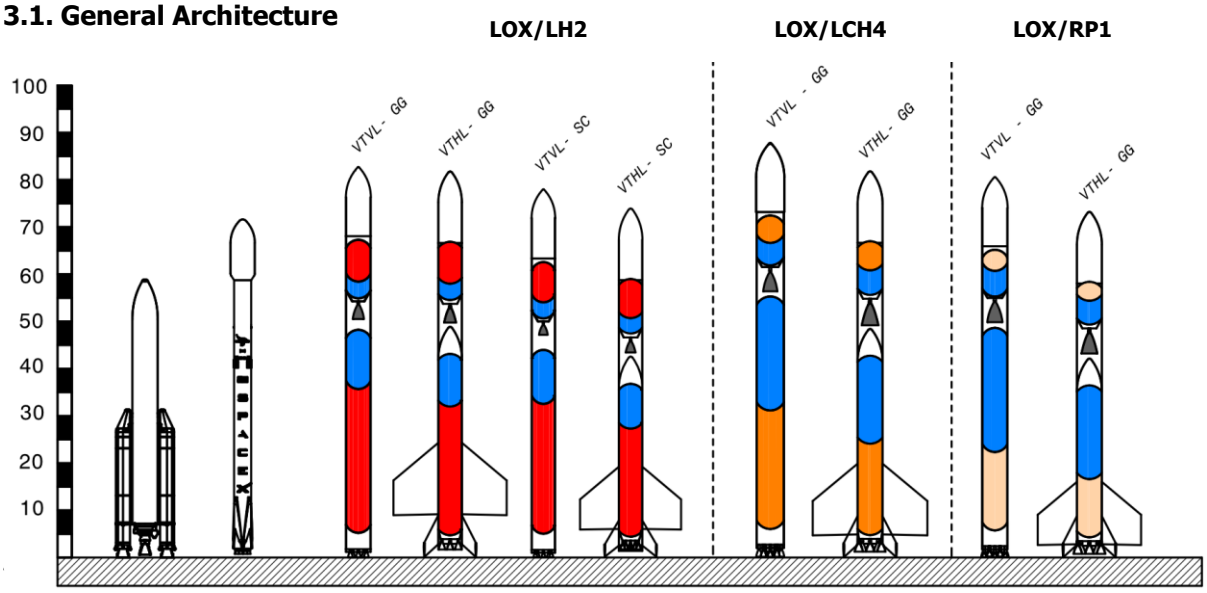

Fig 4. Size and architecture of a selection of analyzed configurations. LOX=blue, LH2=red, LCH4=orange, RP1=peach, [2]

The basic architecture and geometry of some analyzed configurations is shown in Fig 4 in relation to the operational launchers Ariane 5 and Falcon 9. All analyzed configurations use tandem staging. For both VTVL and VTHL an interstage structure is required between the lower and upper stages. Its length is influenced by the length of the upper stage engine and in case of VTHL also the first stage nose structure. Nose structure length is set to 7 m for all VTHL configurations. Comparing the overall geometry from the point of view of fuel and engine cycle choice the excessive dimension of upper stage engines in case of gas generator hydrocarbon configurations stands out. Upper stage engine expansion ratio is fixed to ε=120 for all studied variants. Due to the lower efficiency of methane and kerosene stronger and bigger upper stage engines have to be used. The upper stage engine exit diameter in case of the VTHL kerosene configuration is 3.37 m compared to 2.1 m in case of hydrogen staged combustion. This has an influence on interstage structure length. Stage diameters are between 5.0 and 6.0 m and overall configuration size is below 90 m.

3.1.1. VTVL Recovery Hardware

The VTVL first stages have to be equipped with hardware to enable the safe recovery of the first stage. Since the first stage shall be controllable not only in the exoatmospheric part of the return trajectory (with RCS) but also in the aerodynamic part, aerodynamic control devices are necessary.

Furthermore, the landing of the first stage requires some kind of landing gear or landing legs. This study's VTVL launchers' fins and landing legs masses are calculated by scaling the respective masses of the Falcon 9 with the analyzed launchers' dry mass. The masses of the Falcon 9 recovery hardware such as grid fins and landing legs masses are estimated using in-house tools and reverse engineering, see [10].

3.1.2. VTHL Reusable First Stage General Architecture

The general lay-out of a VTHL reusable first stage is shown in Fig 5 exemplified by the H205 stage using the In-Air-Capturing return mode. The LOX tank is shown in blue, while the LH2 tank is shown in red. All VTHL stages are equipped with a single delta wing and a V-tail. The single delta wing uses an RAE 2822 airfoil and has a leading edge sweep angle of 40 degrees. The chord lengths of the main wing and V-tail are functions of the stage length. Identical ratios of chord length to overall stage length are used for all configurations. Several aspects have an influence on the stage diameter: the dimensions of the payload to be transported, the accommodation of first stage engines and the desired length to diameter ratio of the first stage. The first two aspects are setting lower limits for the stage diameter. For VTHL configurations a length to diameter ratio of 9 is considered desirable for the winged reusable first stage for aerodynamic stability and trimmability reasons. A body flap and wing flaps are used for aerodynamic control. The body flap is used exclusively in the hypersonic regime and is deflected only downward. The minimum stage diameter considered for the presented VTHL configurations is 5.0 m - the nose segment radius 0.5 m. In case of FB as return mode air-breathing engines are located in the nose segment and an additional non-integral fly back fuel tank is placed behind the main, integral LH2 tank, see Fig 6. The selected air-breathing engines are modified EJ200 of MTU Aero Engines without afterburner. They can be operated with hydrogen and have a high specific thrust and thrust to weight ratio, [11]. Between four and six engines are used on FB stages.

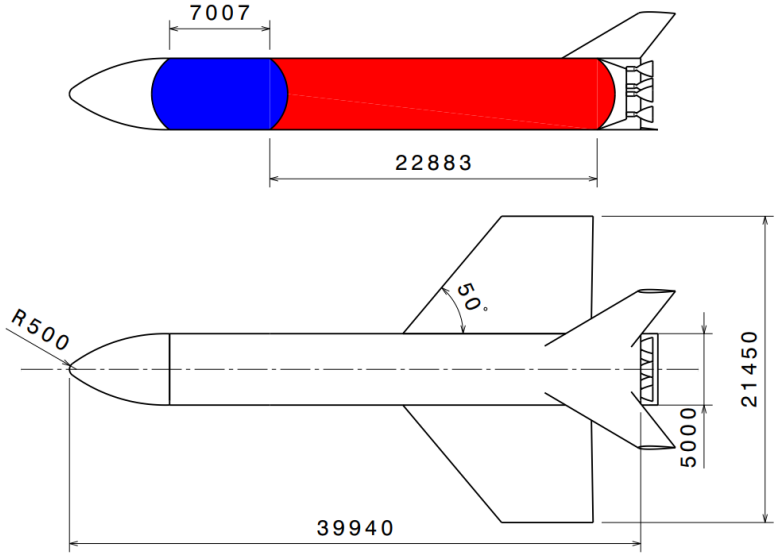

Fig 5. IAC H205 VTHL reusable first stage, LOX=blue, LH2=red

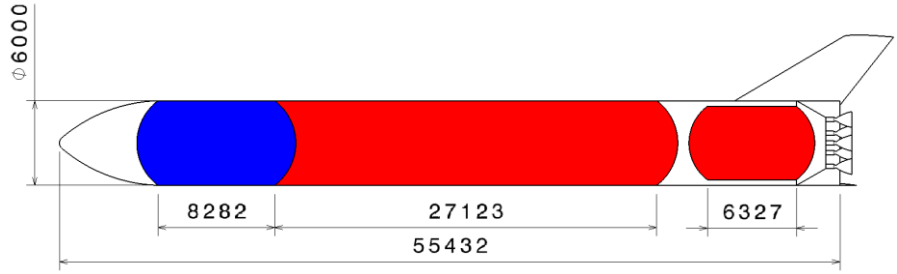

Fig 6. FB H350 VTHL reusable first stage, LOX=blue, LH2=red

3.2. Mass Modelling and Structural Analysis

For mass model definition a combination of empirical methods and preliminary structural analysis based on selected load cases and structural concepts is used. The empirical mass estimation methods are based on stage loads and masses as well as geometrical parameters of the respective component. For structural analysis beam theory is used. Masses of major structural elements as tanks, inter stage structures and thrust frames are obtained by structural analysis whereas empirical methods are applied for the majority of the remaining elements of the mass models. In particular the VTHL first stages wing is sized with empirical methods. Dimensioning parameters are lateral acceleration, stage dry mass as well as wing area, span and thickness. Load cases considered for structural analysis have been limited to ascent load cases.

The following load cases are taken into account for structural analysis:

- Maximum dynamic pressure
- Maximum product of dynamic pressure and AoA (q*alpha)
- Maximum acceleration
- Launch pad in presence of wind loads, launcher full and pressurized
- Pad release

Tanks are modelled as stringer-frame stiffened common bulkhead tanks from aluminum alloy AA2219. Tank pressures are between 3 and 4 bars. Aerodynamic forces are computed with empirical methods. A safety factor of 1.25 is applied.

3.3. Trajectory Simulation and Optimization

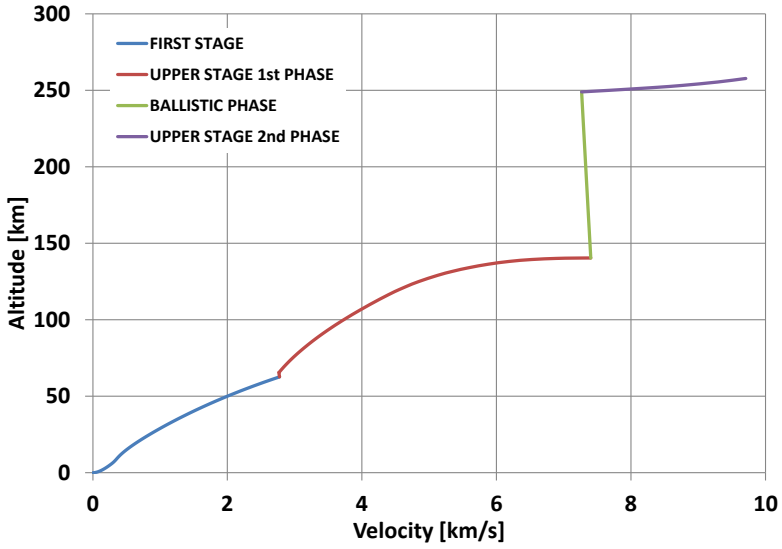

Fig 7. Typical two-stage-to-orbit ascent trajectory (VTHL)

Ascent trajectory optimization for both VTVL and VTHL configurations is performed with a direct method and is based on Sequential Quadratic Programming (SQP). The payload mass delivered to orbit is the optimization objective while pitch rate, thrust angle (w.r.t. velocity), bank angle and thrust throttling are possible control variables. Furthermore additional constraints can be defined. For the present study only pitch rate and thrust angle are used as controls. Axial acceleration is limited to 50 m/s^2. Rocket engines are throttled upon reaching this boundary. It is important to note that due to the requirement that the line of apsides of the GTO ellipse has to be in the equatorial plane upper stage flight is split into two thrust phases with a ballistic phase in between. The initial part of the ascent thus consists of the first stage thrust phase followed by the first thrust phase of the upper stage and allows reaching an intermediate orbit that is followed until crossing the equator. There the upper stage is reignited and apogee reaches GEO altitude. Only the first part of the ascent towards the intermediate orbit is optimized, the second upper stage thrust phase is simulated. The intermediate orbit has a perigee altitude of 140 km, an apogee altitude of 330 km and an inclination of 5.9°. An example of an ascent trajectory is shown in Fig 7. Second phase upper stage delta velocity is 2.4 km/s.

3.3.1. VTVL Descent Trajectories

The VTVL first stages are supposed to land on a drone ship or a similar floating device in the Atlantic Ocean. The descent trajectory is optimized with respect to minimum propellant required without violation of the boundaries. No specific landing site coordinates are defined so that the optimization tool can find the optimal landing site for each launcher and separation velocity. Furthermore, specific landing conditions are prescribed that have to be fulfilled:

- Landing Flight Path Angle: 90° ± 2°
- Landing Velocity: 0 m/s – max. 2.5 m/s
- Landing Altitude: 0 m ± 10m

The following constraints are taken into consideration for VTVL descent trajectories:

- Dynamic pressure < 200 kPa
- Estimated heat flux < 200 kW/m² with respect to a nose radius of 0.5 m
- Lateral acceleration < 3 g

A more detailed discussion and justification can be found in [2].

3.3.2. VTHL Ascent, Descent and Fly-Back Trajectories

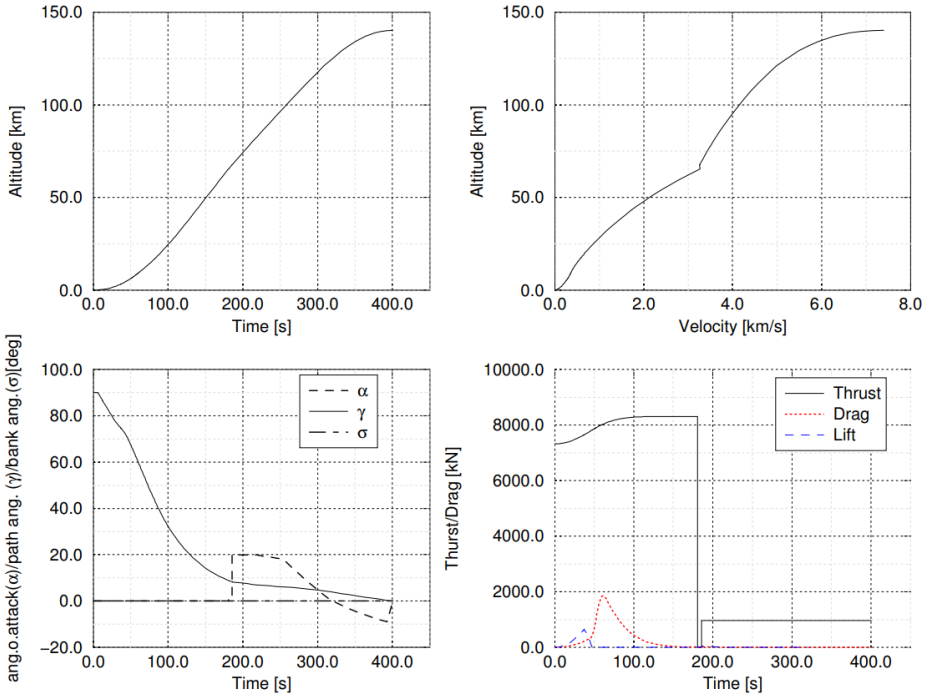

Fig 8. Ascent trajectory of H350 H58 FB configuration

The ascent trajectory of the VTHL reusable first stages is on the one hand optimized with the objective of maximum payload to target orbit, on the other hand the trajectory is constrained taking into account the peak thermal loads during atmospheric reentry. In particular it is attempted to lower the flight path angle at separation by increasing the pitch rate as long as dynamic pressure at separation is below 1 kPa and upper stage thrust angle (w.r.t. velocity) is able to balance out the higher pitch rate. This approach results in small losses of payload mass but significantly reduces the thermal loads during the subsequent reentry phase. In Fig 8 the ascent trajectory of the H350 H58 FB configuration is shown. Flight path angle at separation is below 10 degrees while thrust angle is going up to its maximum allowed value of 20 degrees right after first stage separation. Thrust-to-weight ratios of expendable upper stages at beginning of the first thrust phase are higher than one.

In contrast to the VTVL and VTHL ascent trajectories no reentry trajectory optimization is done for the VTHL reusable first stages. The VTHL reentry trajectories are calculated using quasi-optimal flight control methods. Equations of motion in four degrees of freedom (translation and pitch rotation) are solved. Control of normal acceleration is achieved by variation of angle of attack. As an example time

histories of angle of attack, bank angle (absolute magnitude) and normal acceleration for the H275 FB reusable first stage are shown in Fig 9. After separation angle of attack is increased to a value of 40 degrees. When entering denser layers of atmosphere angle of attack is reduced to limit the normal acceleration to 4 g. Bank angle is varied to initiate a turn and achieve the desired heading towards the launch site. Maximum bank angle is limited to 50 degrees. The beginning of the turn is chosen in order to not excessively increase mechanical and thermal loads during reentry. A more detailed description is given in [12]. Following the atmospheric reentry and turn air-breathing engines are used for a powered return to launch site. The amount of fuel required for the subsonic return flight depends on the stage mass, the distance to be travelled, the efficiency of the air-breathing propulsion system, the aerodynamic performance of the fly-back booster in the subsonic regime as well as the flight Mach number and altitude. Distance to launch site is increasing with first stage separation velocity and among the FB configurations analyzed the one with the highest ascent propellant loading is the most demanding in terms of fly-back fuel mass.

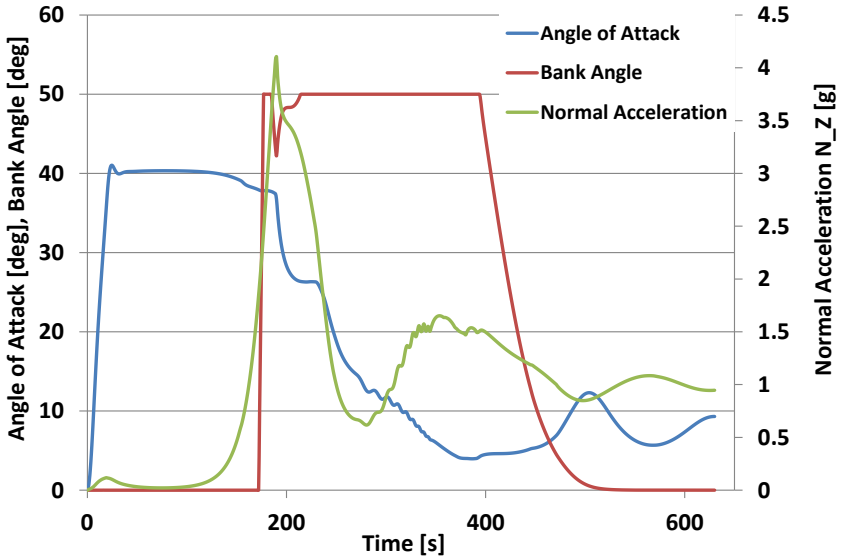

Fig 9. AoA, bank angle and normal acceleration during H275 reentry

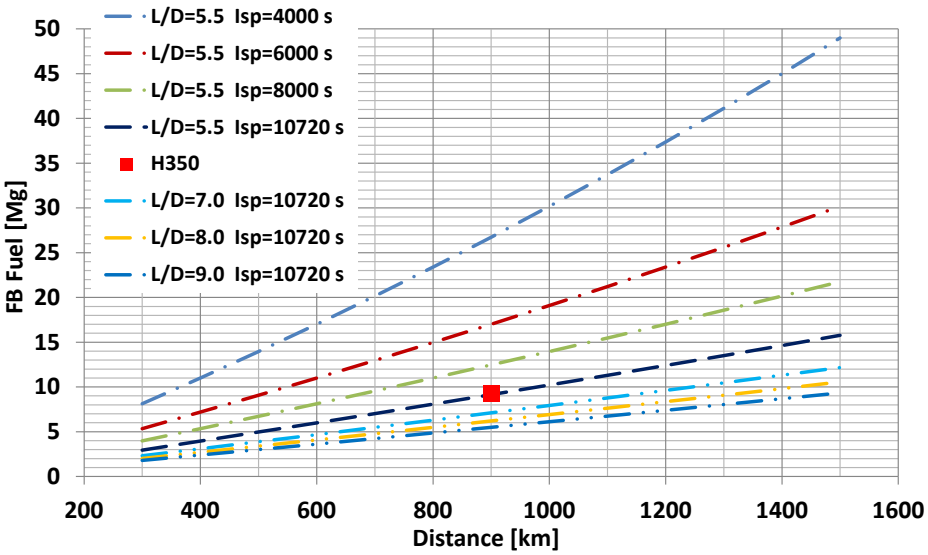

Fig 10. FB fuel mass as function of distance to launch site

The specific impulse of air-breathing engines depends on the type of fuel. While kerosene would be a classic choice its specific impulse is in the area of 4000 s only whereas hydrogen potentially offers a specific impulse of more than 10000 s for typical turbofan engines at subsonic Mach numbers. For all analyzed FB configurations hydrogen has been chosen as fuel for air-breathing engines. From the

point of view of pure subsonic aerodynamic performance a straight, high aspect-ratio wing would be advantageous. However this is not realistic for an RLV stage with a fixed wing. The analyzed single delta wing fly-back stages have L/D ratios between 5 and 6 at subsonic Mach numbers. For the H350 reusable first stage the distance to launch site is 900 km and a fuel mass of 9200 kg is consumed. The calculation of the return trajectory is done by solving 4 DoF equations of motion (translation and pitch rotation). Optimal velocity and altitude profiles are followed to minimize fuel consumption per range. Centre of mass changes due to fly-back fuel consumption are taken into account. Averaged L/D ratio and air-breathing engines specific impulse are at 5.5 and 10720 s. In Fig 10 the Breguet range equation at constant altitude and Mach number is used to visualize the effects of propulsion efficiency and aerodynamic performance. The constant altitude and Mach are chosen equal to averaged values along the calculated H350 trajectory of 6 km and Ma 0.48. The glide ratio is varied between 5.5 and 9.0 whereas engine efficiency is varied from 10720 s to 4000 s. The mass employed is the one of the H350 FB stage at the end of its return flight.

3.4. Modelling of Aerodynamics and Aerothermodynamics

Ascent aerodynamics both for VTVL and VTHL is modelled with empirical, DATCOM like methods for simple fuselage wing combinations. Lift, drag and pitch moment coefficients as a function of angle of attack and Mach number in the subsonic, supersonic and hypersonic regimes are calculated. Methods for fuselage aerodynamics are based on slender body theory. Wing aerodynamics is based on empirical lifting line methods. The trimmed glide ratio of the H205 reusable first stage at subsonic Mach numbers is shown in Fig 11. A maximum lift-to-drag ratio of 5.7 is reached at an angle of attack of about 7 degrees. A wing flap deflection of -5 degrees (upward) is required for trimming at this angle of attack for maximum L/D.

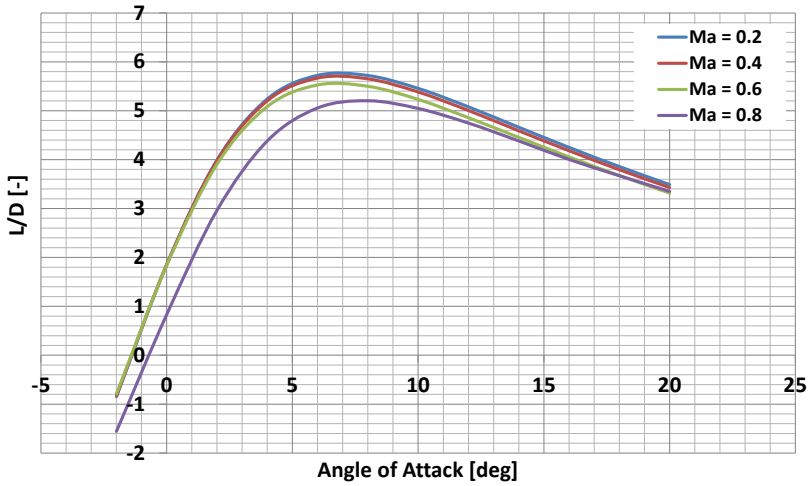

Fig 11. Glide ratio (trimmed) of H205 first stage

Descent aerodynamics for VTVL is as well modeled with empirical methods whereas descent aerodynamics for the winged VTHL first stages is analyzed with empirical methods in subsonic and supersonic regimes and with a surface inclination tool in the hypersonic regime. This program is based on surface inclination methods applicable at high Mach numbers and takes into account high temperature effects. Apart from aerodynamic coefficients as functions of angle of attack and Mach number temperature and heat flux distributions can be obtained. Surface temperature is user specified or calculated based on the assumption of radiation adiabatic equilibrium.

3.4.1. VTHL Aerothermal Loads and TPS Sizing

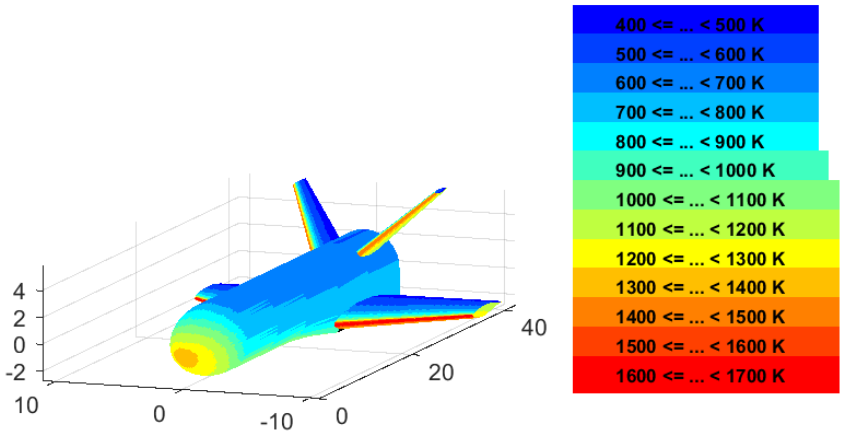

Fig 12. Temperature areas and TPS material distribution for a VTHL first stage, dimensions in m, FRSI (400-600 K), AFRSI (600-900 K), TABI (900-1400 K), AETB (1400-1600 K), CMC (1600-1700 K)

The Thermal Protection System (TPS) is a crucial component for VTHL configurations. In the frame of the current study the mass of the thermal protection system is estimated based on the selected TPS materials and the thermal loads experienced during atmospheric reentry. Fig 12 shows a temperature distribution visualizing the highly loaded nose stagnation area and wing and tail leading edges in orange and red. The VTHL first stages discussed in this work employ TPS materials such as Space Shuttle type Flexible Reusable Surface Insulation (FRSI), Tailorable Advanced Blanket Insulation (TABI) and Alumina Enhanced Thermal Barrier (AETB) ceramic tiles as well as ceramic matrix composites (CMC) for highly loaded areas. A more detailed description of these materials can be found in [13]. The external thermal loads are determined by an aerothermodynamic code for the hypersonic regime. Following the determination of the external loads and the definition of an allowable temperature below the thermal protection the TPS thickness and mass is iteratively calculated assuming one-dimensional heat transfer.

3.5. Rocket Propulsion

In order to ensure comparability of the designed launchers, generic engines with identical baseline assumptions are needed for the systematic assessment and comparison of future RLV-stages. The selected technical characteristics of these generic engines are oriented towards data of existing types as well as previous or ongoing development projects. The two rocket engine cycles most commonly used in first or booster stages are included in the study:

- Gas-Generator cycle
- Staged-Combustion cycle

The main combustion chamber (MCC) pressure is commonly set to 12 MPa for the gas-generator type. This pressure is not far from the useful upper limit of this cycle but is assumed necessary to achieve sufficient performance for the RLV stages. Europe has considerable experience in this range with Vulcain 2 operating at 11.7 MPa. In the case of the staged combustion engines, the MCC pressure is fixed at 16 MPa. This, from a Russian or US perspective, moderate value has been chosen considering the limited European experience in closed cycle high-pressure engines. Nozzle expansion ratios in the first stage are selected according to optimum performance but also requirements of safe throttled operations when landing VTVL stages. For the first stage of the VTVL configurations the engine is computed for expansion ratios of 20 for gas generator types and 23 for the staged combustion variants. This value allows throttling while still retaining sufficient nozzle exit pressure to prevent flow separation within the nozzle. Since the VTHL configurations do not land vertically, the expansion ratio is set to 35 for both gas generator and staged combustion engines. The upper stage engines are derived from the first stage engines with the only difference being the expansion ratio. Its value is set to 120 as a reasonable first assumption and taking into account interstage structure length requirements.

Table 1: Rocket propulsion engine data

Propellants	*LOX/RP-1*			*LOX/LCH4*			*LOX/LH2*					
Stage	**1st**		**2nd**	**1st**		**2nd**	**1st**				**2nd**	
Cycle	**GG**	**GG**	**GG**	**GG**	**GG**	**GG**	**GG**	**GG**	**SC**	**SC**	**GG**	**SC**
ε	**20**	**35**	**120**	**20**	**35**	**120**	**20**	**35**	**23**	**35**	**120**	**120**
Engine MR [-]	2.25	2.25	2.25	2.5	2.5	2.5	6	6	6	6	6	6
Sea level Isp [s]	279	267	-	289	276	-	366	351	394	386	-	-
Vacuum Isp [s]	310	320	338	320	331	348	406	418	428	434	440	457
Engine T/W [-]	112	113	92	98	99	83	98	96	74	72	82	70

All preliminary engine definitions have been performed by simulation of steady-state operation at 100% nominal thrust level using the DLR tools LRP (Liquid Rocket Propulsion) and NCC (Nozzle Contour Calculation) as well as the commercial tool RPA (Rocket Propulsion Analysis). Any potential requirements specific to transient operations or deep-throttling are not considered in this early design study. Common baseline assumptions of all generic engines are discussed in [14]. Turbine entry temperature (TET) is set around 750 K and kept in all cases below 800 K to be compatible with the increased lifetime requirement of reusable rocket engines. Further, all engines considered in this study are designed with regeneratively cooled combustion chambers and regenerative or dump-cooling of the downstream nozzle extensions. The results based on these assumptions are shown in Table 1. Detailed information on the respective engine modelling is given in [3] and [14].

3.6. Propellant Supply System

The propellant supply system including feedlines, fill/drainlines and the pressurization system was modelled using an in-house tool. This program is able to calculate the respective masses for these systems by calculating the propellant and pressurizing gas flow throughout the whole mission and thus sizing the required hardware. Autogenous pressurization is assumed for all configurations except the LOX/RP-1 systems. Here the RP-1 tanks are pressurized with helium. The tool also calculates the mass of the cryogenic insulation of the tanks. It is important to note that insulation was only considered a necessity in the case of LOX/LH2 launchers due to the low temperature of LH2. In the case of hydrocarbon launchers no insulation is used, since it adds mass and it is technically feasible to fly cryogenic propellants without insulation (e.g. Falcon 9 with LOX/RP-1). More information can be found in [2].

4. Comparison of Configurations

4.1. VTHL and VTVL Mass

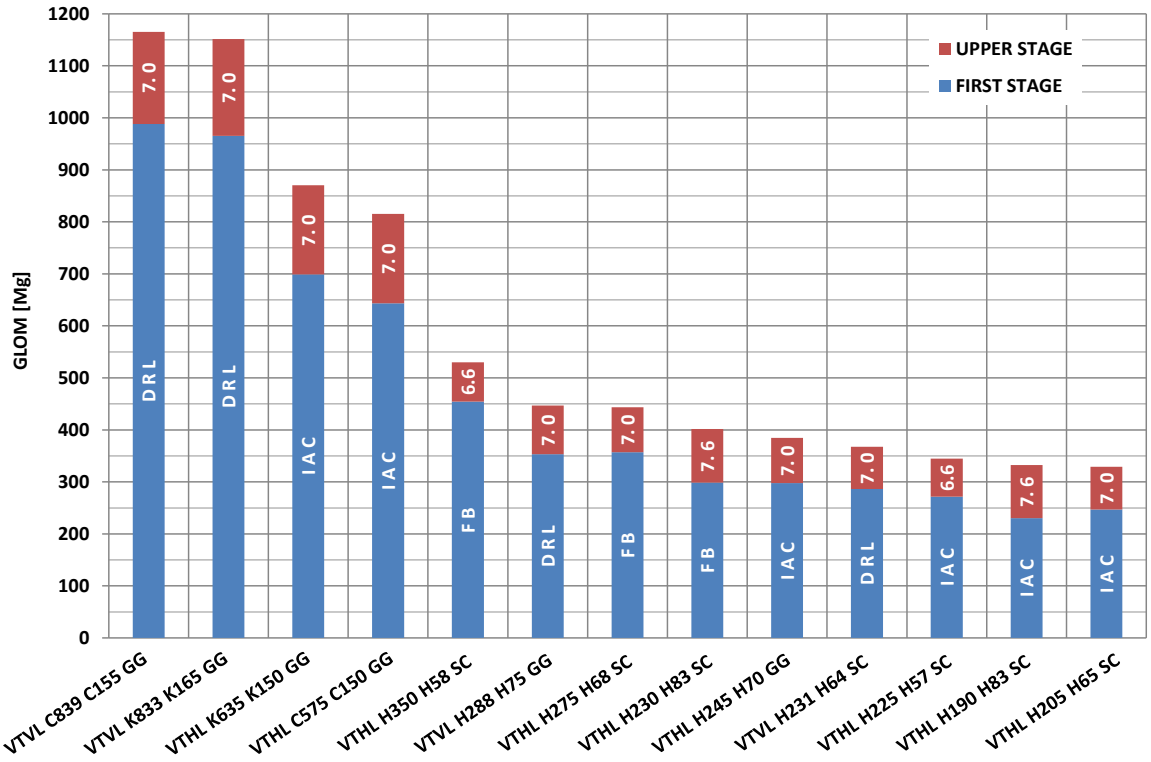

Fig 13. Gross lift-off mass of analyzed configurations

To begin with overall Gross Lift-Off Masses (GLOM) of all analyzed configurations are shown, see Fig 13. The configurations are ordered by decreasing overall lift-off mass also making the distinction between reusable first stage and expendable upper stage lift-off mass. A GLOM range from 1160 Mg down to 330 Mg is covered. First stage return method and upper stage delta velocity in km/s are specified. The configuration nomenclature is specifying whether the specific variant is VTVL or VTHL, the type of fuel and ascent propellant mass in Mg (H=Liquid Hydrogen, C=Liquid Methane, K=RP1) and the rocket engine cycle (SC=Staged Combustion, GG=Gas Generator).

It is remarkable that VTVL down range landing methane and kerosene configurations are by far the heaviest launchers. They are followed by methane and kerosene VTHL In-Air-Capturing configurations. These first four configurations do have the same upper stage delta velocity of 7.0 km/s and VTVL down range landing is considered to be corresponding to VTHL In-Air-Capturing since the winged stage is not flying back to launch site by its own means. Of course the first focus of explanation is the efficiency of methane and kerosene engines. As specified in Table 1 the vacuum specific impulse of e.g. methane and kerosene upper stage engines analyzed for this study is just 348 and 338 s respectively. On the other hand the number of stages is in general fixed to two for all configurations considered within this study. It is known that the theoretical optimal number of stages is in tendency proportional to delta velocity and inversely proportional to average propulsion efficiency. Thus with the target orbit being a GTO and the delta velocity being relatively high these configurations having a relatively low specific impulse and being two stage systems are in a way handicapped w.r.t. launchers with more efficient propulsion systems and the resulting configurations become very heavy compared to systems employing higher Isp engines. Still there is also a significant difference in GLOM between VTHL and VTVL hydrocarbon configurations in general. This can be explained by the fact that for VTVL rocket engines are used both for the ascent and descent of the reusable first stage. Thus the first stage is bringing up a higher delta velocity as compared to VTHL configurations. The delta velocity performance of RLV stages is shown in Fig 14 and VTVL stages delta velocity is more than 1 km/s higher than the one of VTHL stages. Efficiency of rocket engines obviously has to play a higher role for VTVL configurations. On the lower end of the GLOM range

in Fig 13 In-Air-Capturing VTHL hydrogen staged combustion configurations with lift-off masses of around 330 – 340 Mg can be found. With upper stage vacuum specific impulses of more than 457 s they are both using the most efficient propulsion and do not require to return to the launch site with their own propulsion means. Fly-back configurations show an increase of total GLOM with decreasing upper stage delta velocity due to the disproportionate increase of first stage mass including fly-back fuel tanks, air-breathing engines and fly-back propellant. So the fly-back configuration with 7.6 km/s upper stage delta velocity does have a GLOM of 400 Mg whereas the one with 6.6 km/s has a GLOM of around 530 Mg. In contrast to that no significant GLOM increase can be observed for IAC hydrogen staged combustion launchers.

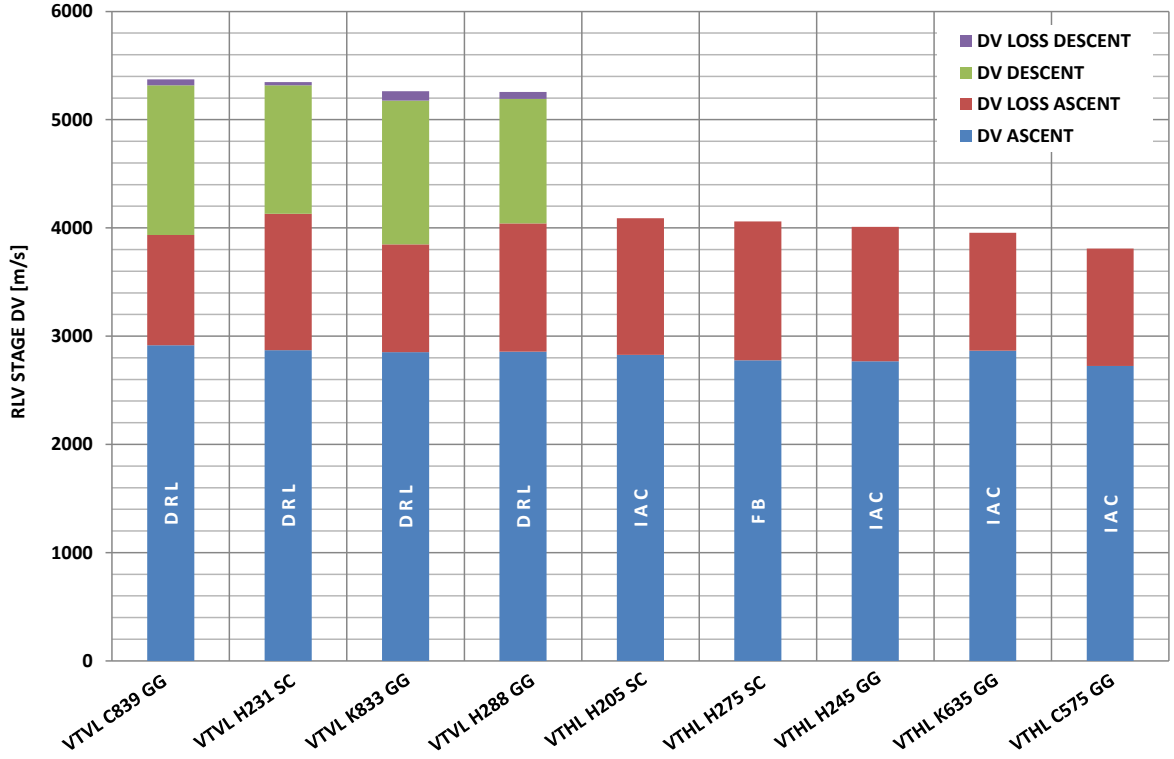

Fig 14. RLV stage delta velocities

Following the discussion of GLOM the first stage dry mass is compared in Fig 15. The dry mass of the first stages is split into rocket engine mass and remaining stage mass (including air-breathing propulsion for FB stages). The relative fraction of engine mass and remaining stage mass is shown along with first stage structural index. Structural index is calculated as first stage dry mass without rocket engines divided by the first stage total propellant mass. Within the dry mass range of 36 to 88 Mg the VTHL fly-back and both VTVL and VTHL hydrocarbon configurations are the heaviest. In contrast to that the lightest configurations are both VTVL and VTHL hydrogen staged combustion configurations not returning to launch site. Structural index of hydrogen staged combustion FB configurations is increasing from 20.4 to 21.1 % with decreasing first stage ascent propellant load whereas the rocket engine mass fraction almost stays the same at 15 to 16%. In comparison to that the hydrocarbons structural indices are significantly lower and range from 5.4 to 7.6 % only. On the other hand the rocket engine mass fraction is at 26 to 27 %. The high engine mass fraction in case of hydrocarbons is first due to more compact, more efficient stage structures (expressed in terms of structural index), in addition to that the lower propulsion efficiency together with the top level requirement of equal thrust-to-weight ratio at launch leads to bigger and heavier engines and this despite their higher engine thrust-to-weight ratios (see Table 1). For example the absolute mass of C839 rocket engines is 20.6 Mg compared to 13.1 Mg of H350. Knowing that rocket engines are significantly more expensive than other stage components as e.g. tanks this is important if dry mass is considered to be a figure of merit for RLV stage comparison. That said for those configurations not returning to launch site with their own means not only do the hydrocarbons have highest dry masses, they also have highest rocket engine fractions.

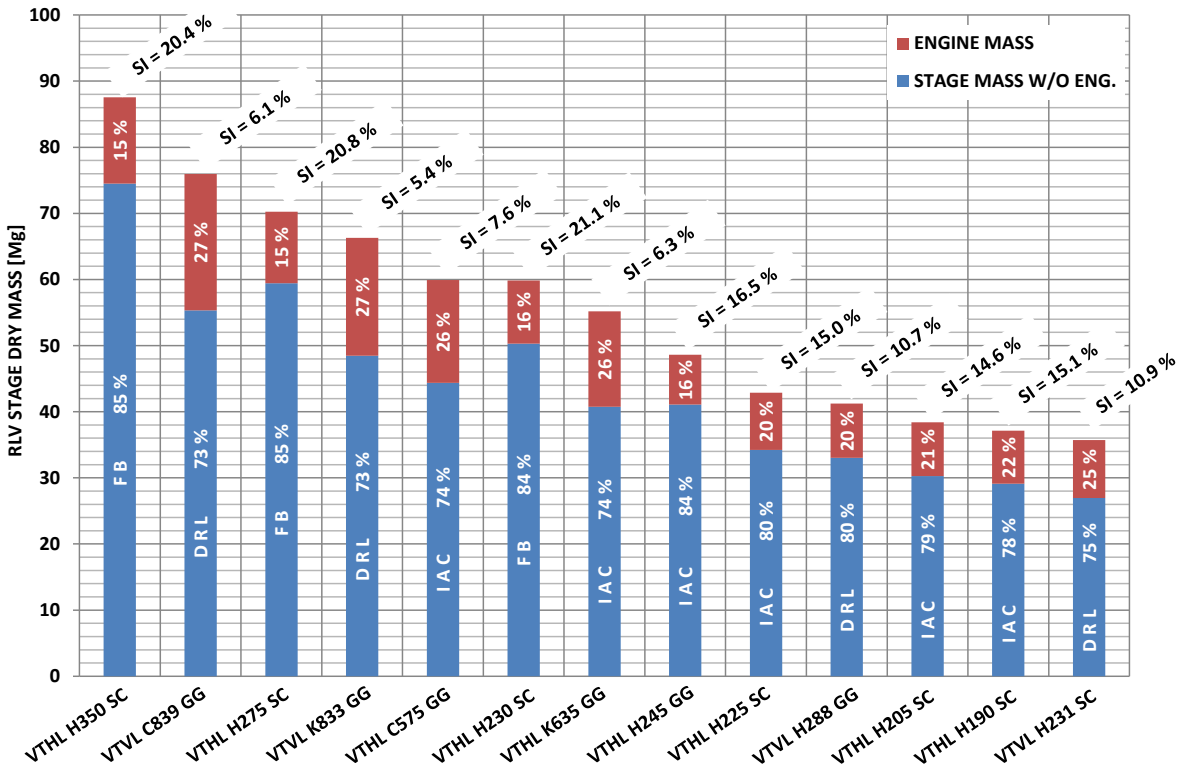

Fig 15. RLV stage dry mass

Consistent with the discussion of GLOM the VTVL methane and kerosene configurations do have a higher dry mass than the VTHL hydrocarbon launchers. Both for VTVL and VTHL methane as the fuel in tendency leading to higher structural indices does have higher dry mass as compared to kerosene. However the difference in structural index is slightly higher in case of VTHL. This is due to the fact that a part of VTHL dry mass as e.g. wing and fins as well as the thermal protection system are scaled with length and depend on stage size. Thus a more compact stage will also have a smaller and lighter wing and fins as well as a smaller surface to be protected by thermal insulation.

The IAC VTHL hydrogen staged combustion configurations show a much smaller dependence on upper stage delta velocity than the FB configurations since no fly-back hardware as tanks, engines and additional subsystems is part of the stage. Their structural indices are all around 15 % and rocket engine fraction is between 20 and 22 %. The slight increase in rocket engine fraction with decreasing stage propellant load is again due to horizontal landing hardware also becoming smaller and lighter. When VTVL and VTHL is compared for hydrogen and same engine cycle as well as upper stage delta velocity we see lower structural indices and higher rocket engine fractions in case of VTVL. Absolute engine masses are 8800 kg (VTVL) vs. 8100 kg (VTHL) for staged combustion and 8200 kg (VTVL) vs. 7600 kg (VTHL) for the gas generator cycle. Still it is remarkable that the ascent propellant mass of VTVL configurations in these cases is higher namely 231 vs. 205 Mg for staged combustion and 288 vs. 245 Mg for the gas generator cycle. This is because of the VTVL drawback of accelerating propellant that later will be used for reentry and landing. This is also true for the comparison of VTHL and VTVL hydrocarbon configurations.

The payload fraction is an indicator of launch vehicle performance. Payload fractions for all analyzed configurations are shown in Fig 16. Note that in this study all launchers have the same design payload mass. However relation of payload mass to gross lift-off mass is considered to be of general interest.

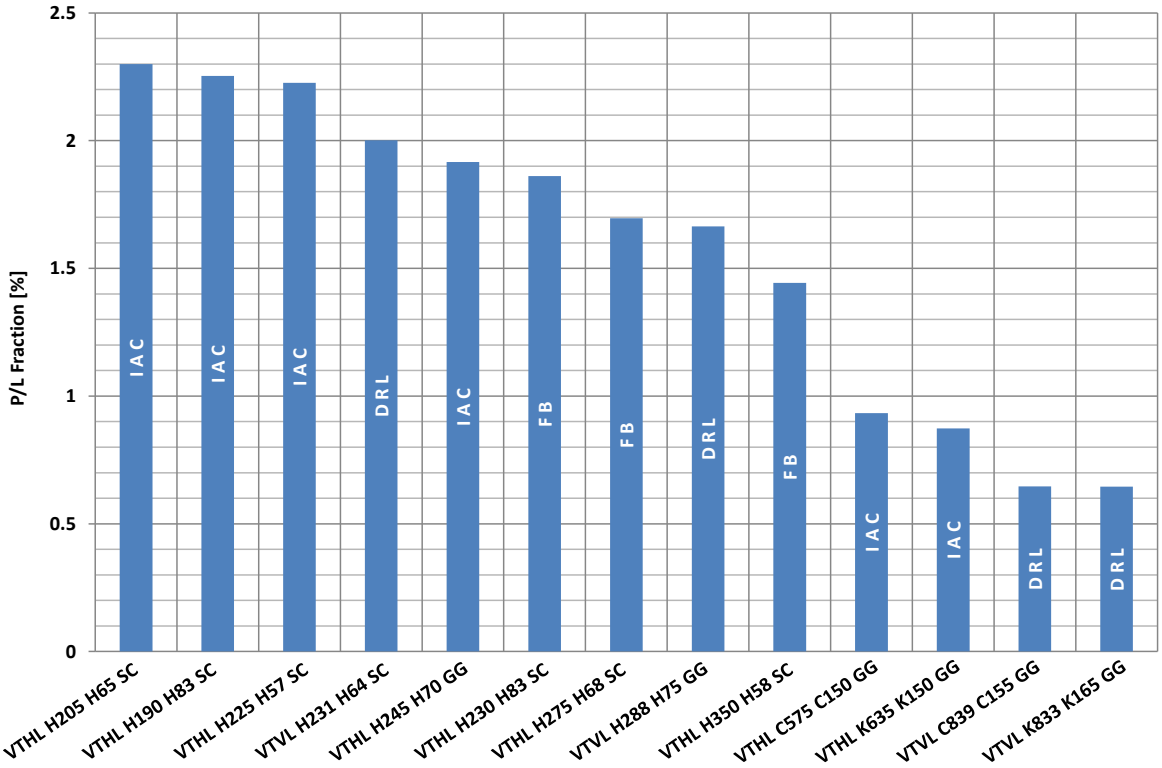

Fig 16. Payload Fraction Ratio

The highest payload fractions of 2.2 to 2.3 % are seen for IAC hydrogen staged combustion configurations. Still the VTVL H231 H64 SC configuration with a payload fraction of 2 % is very close to the hydrogen staged combustion IAC stages. FB configurations have payload fractions of 1.85 to 1.4%. For both VTVL and VTHL the hydrocarbon configurations show the lowest performance indices below 1 %.

4.2. VTHL and VTVL First Stage Descent Trajectories and Loads

Descent trajectories of all analyzed VTVL and VTHL first stages are shown in Fig 17. Altogether four RLV first stages are VTVL configurations and landing down range. They have been designed for an upper stage ΔV of 7.0 km/s. Hydrogen staged combustion and gas generator, methane gas generator and kerosene gas generator propulsion is used. The VTVL configurations altitude over velocity is shown in dashed lines. The VTHL configurations consist of three FB and three IAC stages using hydrogen staged combustion designed for upper stage ΔVs of 6.6, 7.0 and 7.6 km/s. In addition hydrogen, methane and kerosene gas generator configurations have been designed for an upper stage ΔV of 7.0 km/s. Altitude as a function of velocity is shown in Fig 17 from RLV stage separation down to a velocity of 400 m/s since thermal loads critical during reentry will be present in that velocity range. Landing of the VTVL and VTHL stages is not shown and not discussed here. Stagnation point heat flux over time is shown in Fig 18 for all analyzed stages. Stagnation point heat flux is calculated using an empirical relation for a radius of 0.5 m. This is equal to the nose radius of the VTHL first stages.

The FB and IAC VTHL staged combustion stages both have separation velocities from approximately 3.3 to 2.3 km/s. Maximum altitude is below 90 km in all cases. Thus independent of first stage size it is possible to avoid leaving the atmosphere. But for the configurations having high separation velocities this is due to low flight path angles whereas for the smaller ones this is a consequence of the lower velocities. Stagnation point heat flux is proportional to the product of density and the velocity cubed and does reflect the different conditions at the beginning of reentry. As can be seen in Fig 18 the maximum stagnation point heat flux values for FB range from 220 kW/m² for highest separation velocity to 115 kW/m² for the lowest. For IAC a range from 160 to 70 kW/m² is covered. In general IAC configurations are flying higher at the same velocities as compared to FB. This is due

to their lower reentry masses. Wing loading for IAC configurations is in the area of 230 kg/m² whereas in case of FB it varies from 310 to 270 kg/m².

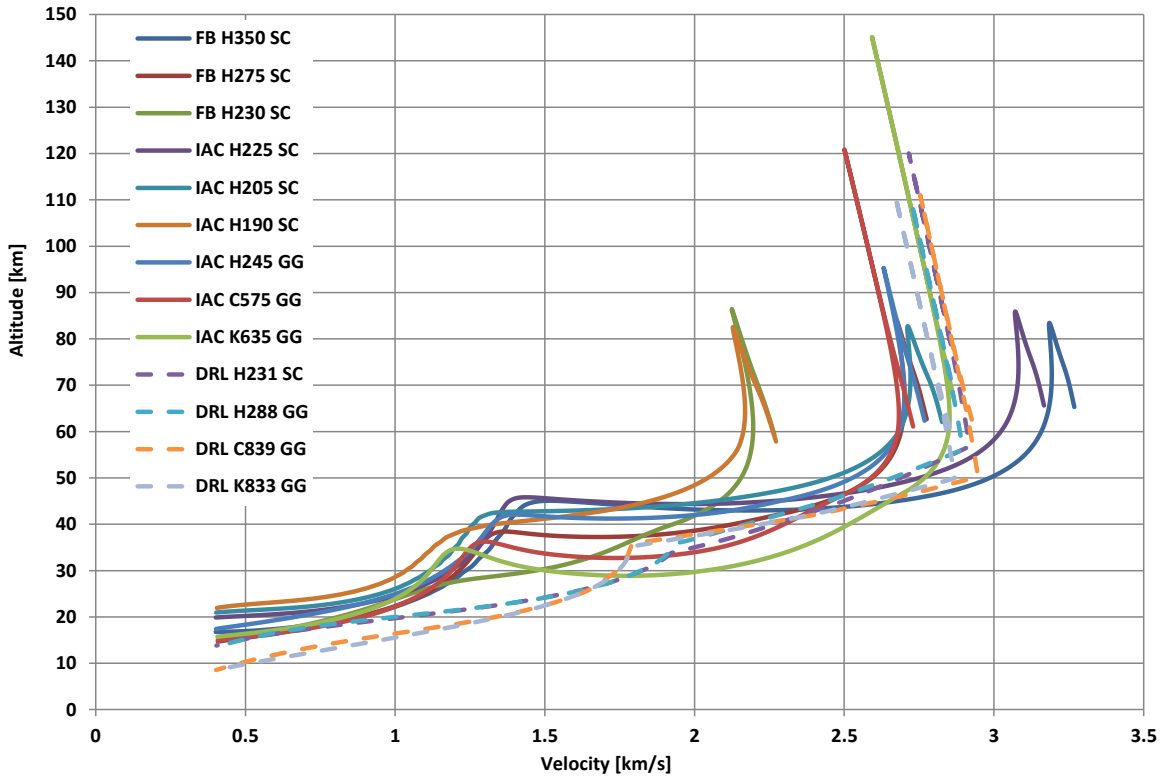

Fig 17. Altitude-velocity map - VTHL and VTVL reusable stages

Among the VTHL configurations with separation velocities of about 2.8 km/s (corresponding to an upper stage ΔV of 7.0 km/s) the IAC K635 GG stage is reaching a maximum altitude of more than 140 km after separation and is flying at significantly lower altitudes than other VTHL stages at velocities between 2.5 and 1.5 km/s. This is due to its very high flight path angle of γ = 22.9° at separation. In contrast to that e.g. the FB H205 stage only has a γ of 11.2° at separation and as a consequence a much shallower trajectory. For K635 a peak stagnation point heat flux value of 295 kW/m² is reached. For methane the C575 separates at a flight path angle of 21° with a resulting thermal load of 200 kW/m². The relatively strong reduction of heat flux in presence of rather similar flight path angles at separation has to do with the propellant combination and is also to be explained by the scaling approach for the reusable first stage wings. Both stages have a diameter of 5.3 m which is a consequence of the requirement of accommodating the rocket engines inside the diameter. However the density of kerosene is higher and stage length is smaller. This results in a wing area increase of 30% for the methane configuration compared to the kerosene stage while reentry masses do differ only slightly. As a consequence the methane stage is flying at higher altitudes and is experiencing lower thermal loads. A further reduction can be observed for the H245 stage that has a γ of 15° at separation and reaches a maximum stagnation point heat flux value of 130 kW/m². The optimization of wing size w.r.t. thermal loads and associated TPS mass would thus be of general interest for this type of vehicles.

The VTVL first stages perform a propulsive reentry. This can be clearly seen in Fig 17 since the reentry burn performed to limit thermal loads during the descent causes a bending of the altitude trend at the beginning of the maneuver. During the reentry maneuver altitude over velocity shows an almost linear behavior in contrast to the VTHL stages. Flight path angle at separation does not vary as much as for VTHL with values between 16° and 18°. In contrast to VTHL the VTVL first stages descent trajectories are optimized with the objective to minimize the descent propellant mass without violation of defined constraints. The respect of the path constraint of 200 kW/m² heat flux is clearly seen in Fig 18. This value is based on Space X Falcon 9 trajectories. Two local heat flux maxima are observed for the VTVL stages. When the defined limit of 200 kW/m² is approached the engines are

fired until the heat flux starts to decrease and the following increase along the non-propulsive part of the descent trajectory (second local peak) does not violate the defined constraint. For VTVL the empirical heat flux estimation is also done for a stagnation point radius of 0.5 m as in the case of VTHL. Still in contrast to VTHL this radius is not necessarily representative of the reentry geometry. Note as well that the heat loads linked to the fact that a VTVL is flying through its rocket engines plume are not considered here. In that case thermal loads are spread over a larger vehicle area due to modifications of the flow field. More details based on CFD computations concerning the aerothermal loads in case of VTVL can be found in [15].

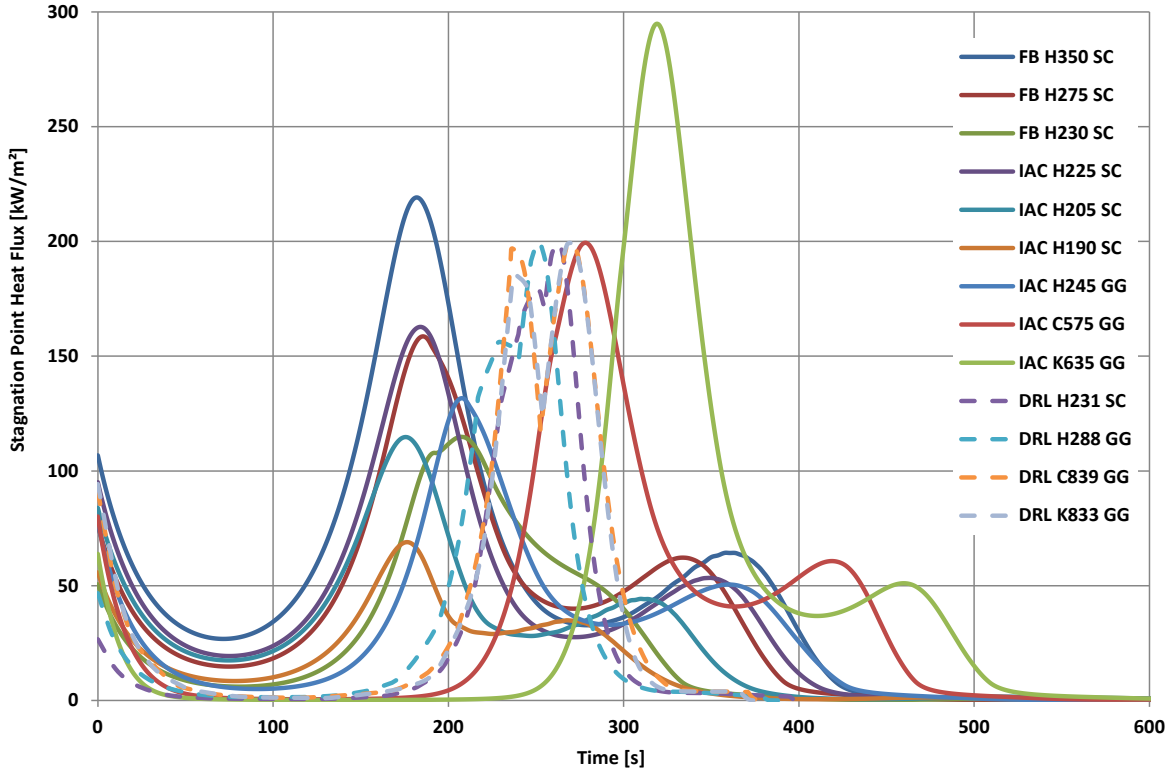

Fig 18. Stagnation point heat flux VTHL and VTVL stages

4.3. Comparison of VTHL FB and IAC Configurations

Fly-back as return option does have the advantage of autonomous reentry and subsonic return flight but has the drawback of additional hardware and fly-back fuel that needs to be carried both during ascent as well as reentry flight resulting in bigger and heavier stages experiencing higher loads during reentry. In-air-capturing avoids the additional fly-back hardware and propellant but has to rely on a towing aircraft that is supposed to tow it back to launch site. In both cases the reentry mass and distance to launch site to be flown by either the autonomous fly-back stage or the mated towing aircraft and IAC stage will have a large impact on the systems involved. Reentry masses of VTHL hydrogen staged combustion configurations over distance to launch site are shown in Fig 19. It can be seen that reentry masses of FB stages are higher than their IAC counterparts by 78 to 134 %. Only a moderate increase of 19 % is observed for the IAC stages reentry mass. In contrast to that FB stage reentry mass does increase by 57 %. The fly-back fuel fraction does increase from 7.8 % for the H230 stage to 11.7 % for the H350 configuration. Distance to launch site grows by around 200 km when reusable first stage size is increasing. All FB configurations are using hydrogen staged combustion rocket engines as well as hydrogen as air-breathing engine fuel. The need to return to launch site makes fuel choice and engine efficiency more important for FB stages. And since already for IAC configurations not returning to launch site the hydrocarbon configurations show both highest GLOM and dry masses, see Fig 13 and Fig 15, it can be expected that for less efficient rocket and air-breathing propulsion the difference between FB and IAC would increase even more. Thus use of hydrocarbons for FB stages does not seem to be promising within the assumptions of the current study.

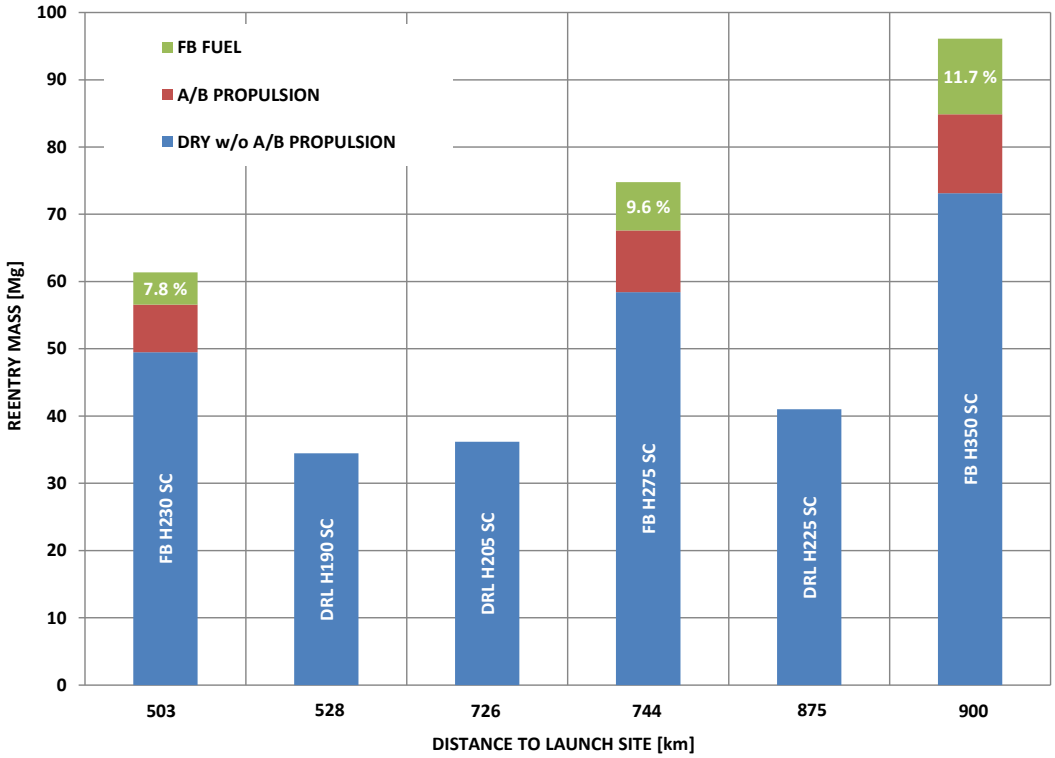

Fig 19. RLV stage reentry mass

4.4. Comparison of VTHL Thermal Loads and TPS Sizing

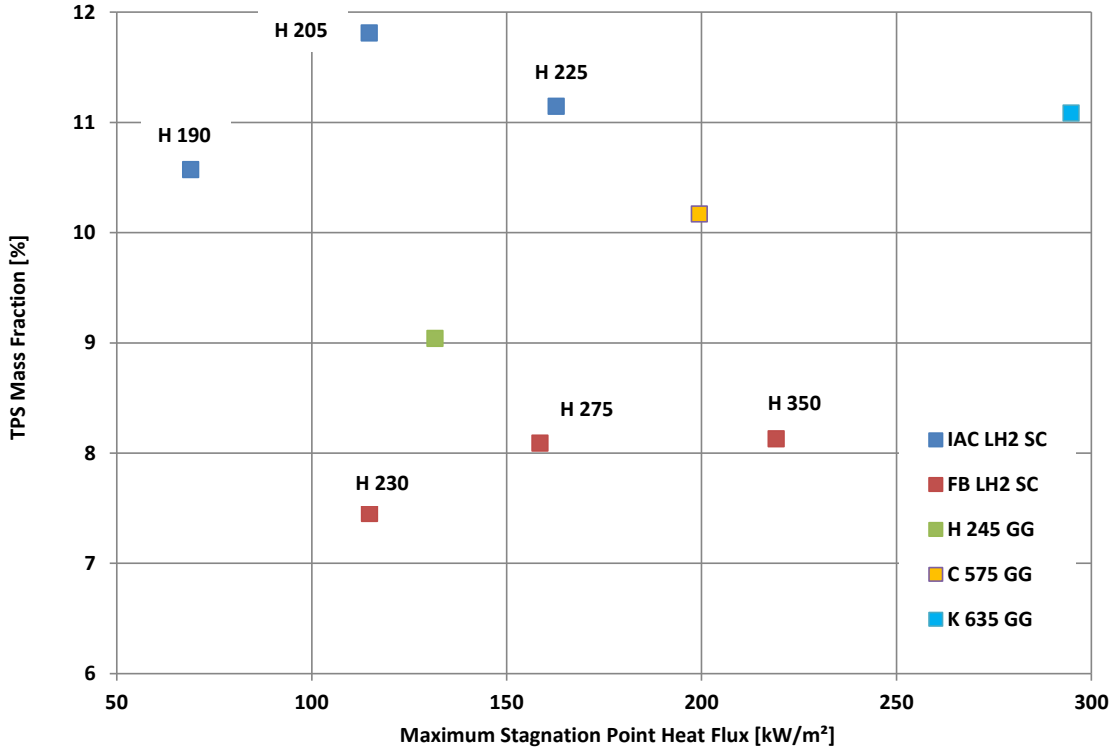

Fig 20. TPS mass fraction for LH2, LCH4 and RP1 GG configurations

Following the discussion of VTHL and VTVL reentry trajectories and loads a more detailed look on VTHL TPS design is taken. Selected trajectories, TPS mass fractions and temperature distributions are presented. The TPS mass fraction for all analyzed VTHL first stages is shown in Fig 20. TPS mass

fraction is understood as TPS mass divided by reusable first stage dry mass. TPS mass fraction is shown in relation to maximum stagnation point heat flux experienced by the stages along their reentry trajectories. A range from 7.5 % for the FB H230 stage to 11.8 % for the IAC H205 configuration is covered. IAC and FB LH2 SC stages are shown for different separation velocities (corresponding to different upper stage ΔVs) while hydrogen, methane and kerosene GG configurations are all designed for an upper stage ΔV of 7.0 km/s.

It is noteworthy that hydrogen SC IAC stages do have very high TPS fractions although thermal loads are rather low. In contrast to that thermal loads for FB stages are higher but TPS fractions are lowest. To a big extent this has to do with the differences in reusable first stage dry mass. The dry mass of e.g. the FB H275 and IAC H205 stages differs by almost a factor of two. On the other hand the absolute TPS mass is higher for the FB configuration by 30 %. The same applies for comparisons within the IAC return method. Here absolute TPS masses of the H205 SC and H245 GG stages differ by less than 3 % whereas the dry mass of the gas generator stage is higher by 27 %. TPS mass fraction within the SC IAC and FB groups is not highest for maximum thermal load. Despite of absolute TPS mass increase due to higher loads and surface to be protected the associated dry mass increase has a bigger effect.

The LH2, LCH4 and RP1 GG stages shown in Fig 20 use different propellant combinations but are designed for the same upper stage ΔV of 7.0 km/s and experience different levels of thermal loads. The maximum stagnation point heat flux for the H245 stage is 130 kW/m², for the C575 200 kW/m² and the K635 experiences a maximum load of 295 kW/m². Due to the thermal loads increase the TPS mass fraction is increasing from 9 % for LH2, 10.2 % for LCH4 to 11.1% for RP1. For these stages relative dry mass difference is below 20 % whereas maximum stagnation point heat flux increases by a factor of 2.3. Thus differences in thermal loads and absolute TPS masses are dominating and leading to the observed increase in TPS mass fraction.

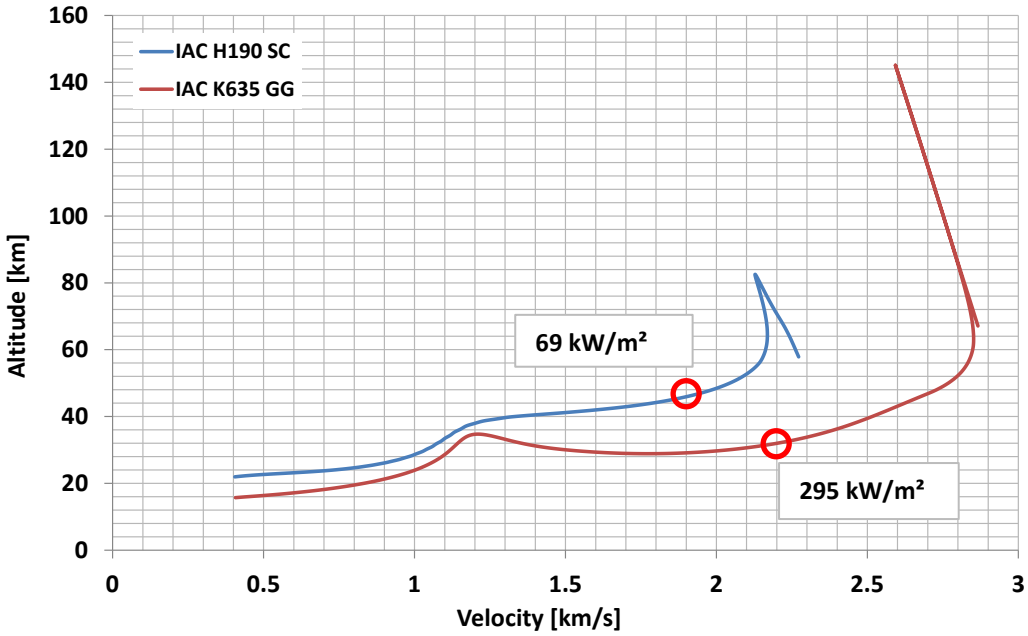

Fig 21. Reentry trajectories of H190 and K635 RLV stages

Trajectories of H190 and K635 first stages are shown in Fig 21. Among the VTHL configurations the H190 stage does have the lowest thermal load whereas the K635 has the highest. The maximum load flight point for the H190 stages is in 47 km altitude, at an angle of attack of 46.7° and a Mach number of 6. For the K635 maximum thermal load is encountered in 32.6 km, at an angle of attack of 13.8° and a Mach number of 7.3. Radiation adiabatic temperature distributions for these flight points are shown in Fig 22 and Fig 23. In case of H190 the overall TPS mass is 3500 kg and 85 % of the TPS mass consists of FRSI and AFRSI, materials for a temperature range of 400 – 900 K. In contrast to that for K635 out of a total of 5300 kg 89 % of the TPS is made out of AFRSI and TABI foreseen for use at 600 – 1400 K.

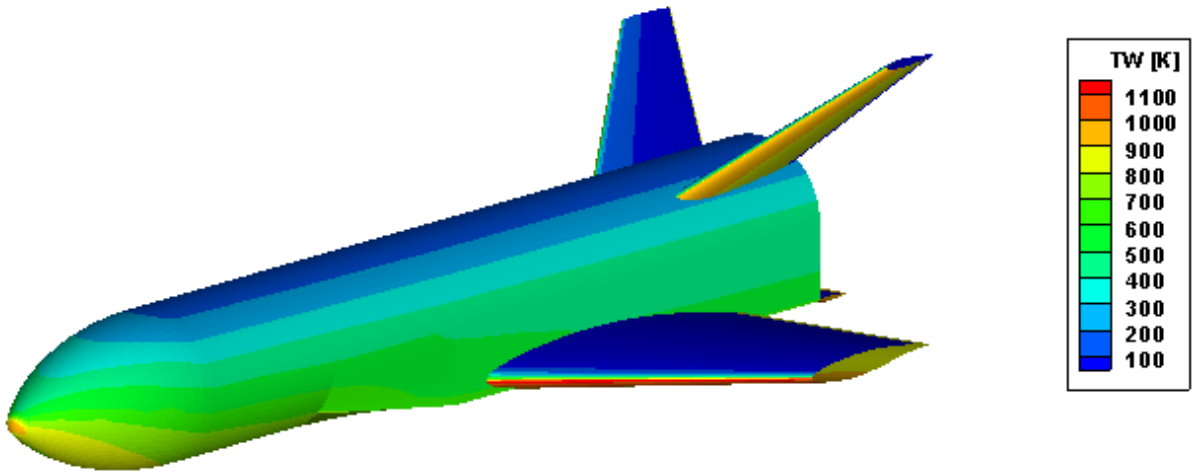

Fig 22. Radiation adiabatic temperature distribution H190 stage, altitude=47 km, AoA=46.7°, Ma=6.0

Surface temperatures for the H190 stage are at around 1000 K in the nose stagnation point region and above 1100 K in the area of main wing and fins leading edges. In case of K635 in the nose stagnation point region a temperature of 1400 K can be seen in Fig 23. For wing and fins leading edges temperatures go above 1600 K.

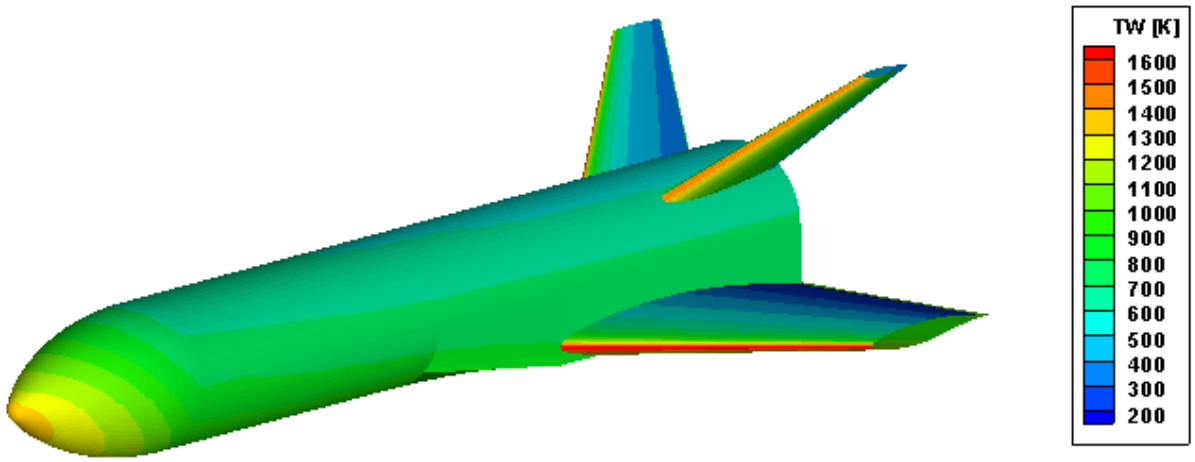

Fig 23. Radiation adiabatic temperature distribution K635 stage, altitude=32.6 km, AoA=13.8°, Ma=7.3

5. Summary and Conclusions

In the frame of the performed analysis 13 partially reusable two-stage launcher configurations have been analyzed with the goal of comparison and evaluation. Both VTVL and VTHL configurations have been considered. Principal study assumptions and requirements common to all analyzed variations have been the delivery of 7500 kg of payload to GTO launching from Kourou and a T/W ratio of 1.4 at launch. Upper stage delta velocities of 6.6, 7.0 and 7.6 km/s have been considered for winged reusable first stages. For VTVL first stages upper stage ΔV has been limited to 7.0 km/s. For VTHL both fly-back stages returning to launch site as well as In-Air-Capturing configurations have been studied. For VTVL only configurations with reusable first stages landing down range of the launch site have been taken into account. Liquid hydrogen, methane and kerosene have been considered as rocket engine fuels.

The lowest gross lift-off masses both for VTVL and VTHL IAC are achieved using efficient hydrogen staged combustion engines. The lowest GLOM is shown by VTHL IAC for an upper stage ΔV of 7.0 km/s. However no big difference can be observed compared to the corresponding VTVL

configuration. The effect of upper stage ΔV variation on VTHL IAC configurations is very small. The lowest reusable first stage dry mass is shown by the hydrogen staged combustion VTVL configuration. For both VTVL and VTHL configurations not returning to launch site the use of hydrocarbon fuels results in highest GLOMs and first stage dry masses. Also rocket engine mass fraction is highest for the hydrocarbon configurations. The impact of rocket engine efficiency is higher for VTVL configurations. This is due to the fact that VTVL first stages ΔV is higher by more than 30 % compared to VTHL first stages. In summary a general, significant advantage of VTHL over VTVL cannot be concluded. The main difference between VTVL and VTHL is that in case of vertical landing the resulting designs feature increased rocket propellant and engine masses while in case of horizontal landing increased dry mass in form of wings, fins and air-breathing propulsion has to be considered. Operational aspects have not been considered in this study.

The thermal loads experienced during reentry are similar for all analyzed VTVL configurations due to the optimization performed but differ in a wide range for VTHL configurations partly due to the study assumptions. But in contrast to VTVL for VTHL stages the thermal protection system is sized based on aerothermodynamic calculations for selected flight points at hypersonic Mach numbers along the reentry trajectory. Thus the loads along the reentry trajectory are reflected in the reusable stage mass model. However the presented comparison of VTVL and VTHL thermal loads is difficult because heat fluxes are determined by an empirical relation and in case of VTVL the reference radius is not necessarily representative of the reentry geometry. This is further aggravated by the fact that for VTVL the effect of rocket engines working during the propulsive phase has not been considered.

Among the hydrogen staged combustion VTHL configurations IAC stages have lower reentry masses and experience lower thermal loads as compared to FB. The difference in reentry mass is increasing with first stage separation velocity which makes the FB stages increasingly less attractive as compared to IAC. However it should be noted that In-Air-Capturing is equivalent to a reusable first stage landing down range of the launch site while among the analyzed vehicles fly-back configurations are the only RLV stages capable of autonomous return to launch site without relying on drone ships or towing aircrafts.

6. Acknowledgements

The authors would like to acknowledge the contribution of everyone involved in the ENTRAIN system study and the design process of the presented partially reusable launcher configurations.

References

1. Dumont, E., Stappert, S., Ecker, T., Wilken, J., Karl, S., Krummen, S., Sippel, M.: Evaluation of Future Ariane Reusable VTOL Booster Stages. IAC-17-D2.4.3, 68th International Astronautical Congress, Adelaide 2017.
2. Wilken, J., Stappert, S., Bussler, L., Sippel, M., Dumont, E.: Future European Reusable Booster Stages: Evaluation of VTHL and VTVL Return Methods. 69th International Astronautical Congress, Bremen 2018.
3. Stappert, S., Wilken, J., Sippel, M., Dumont, E.: Assessment of a European Reusable VTVL Booster Stage. Space Propulsion Conference, Seville 2018.
4. Sippel, M., Manfletti, C., Burkhardt, H.: Long-term/strategic scenario for reusable booster stages. Acta Astronautica, Volume 58, Issue 4, February 2006, pp 209 – 221.
5. Sippel, M., Klevanski, J.: Progresses in Simulating the Advanced In-Air-Capturing Method. 5th International Conference on Launcher Technology, Madrid 2003.
6. Sippel, M., Bussler, L., Krause, S., Cain, S.: Bringing Highly Efficient RLV-Return Mode „In-Air-Capturing" to Reality, 1st HiSST, Moscow 2018.
7. Sippel, M., Stappert, S., Bussler, L.: Systematic Assessment of Reusable First-stage Return Options. IAC-17-D2.4.4, 68th International Astronautical Congress, Adelaide 2017.

8. Bussler, L., Sippel, M.: Comparison of Return Options for Reusable First Stages. AIAA 2017-2137, 21st AIAA International Space Planes and Hypersonic Systems and Technologies Conference, Xiamen 2017.
9. Stappert, S., Wilken, J., Sippel, M., Dietlein, I.: Evaluation of European Reusable VTVL Booster Stages. AIAA Space and Astronautics Forum and Exposition, Orlando 2018.
10. Stappert, S., Sippel, M.: Critical Analysis of SpaceX Falcon 9 v1.2 Launcher and Missions. DLR SART TN-009/2017, 2017.
11. Waldmann, H., Sippel, M.: Adaptation Requirements of the EJ200 as a Dry Hydrogen Fly Back Engine in a Reusable Launcher Stage. ISABE-2005-1121, September 2005.
12. Klevanski, J., Sippel, M.: Quasi-Optimal Control for the Reentry and Return Flight of an RLV. 5th International Conference on Launcher Technology, Madrid 2003.
13. Myers, D.E. et al.: Parametric Weight Comparison of Advanced Metallic, Ceramic Tile and Ceramic Blanket Thermal Protection Systems. NASA TM-2000-210289.
14. Sippel, M., Wilken, J.: Preliminary Component Definition of Reusable Staged-Combustion Rocket Engine. Space Propulsion Conference, Seville 2018.
15. Ecker, T., Zilker, F., Dumont, E., Karl, S., Hannemann, K.: Aerothermal Analysis of Reusable Launcher Systems during Retro-Propulsion Reentry and Landing. Space Propulsion Conference, Seville 2018.